



Published in final edited form as:

*J Am Soc Mass Spectrom.* 2018 March ; 29(3): 481–489. doi:10.1007/s13361-017-1861-2.

## UV Lamp as a Facile Ozone Source for Structural Analysis of Unsaturated Lipids via Electrospray Ionization-Mass Spectrometry

Craig A. Stinson<sup>1,#</sup>, Wenpeng Zhang<sup>1,2</sup>, and Yu Xia<sup>1,2,\*</sup>

<sup>1</sup>Department of Chemistry, Purdue University, West Lafayette, IN, 47907-2084, USA

<sup>2</sup>Department of Chemistry, Tsinghua University, Beijing, China, 100084

### Abstract

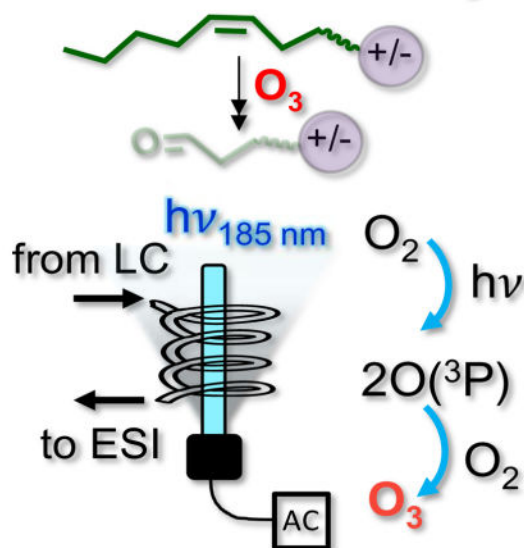
Ozonolysis of alkene functional groups is a type of highly specific and effective chemical reaction, which has found increasing applications in structural analysis of unsaturated lipids via coupling with mass spectrometry (MS). In this work, we utilized a low-pressure mercury lamp (6 W) to initiate ozonolysis inside electrospray ionization (ESI) sources. By placing the lamp near a nanoESI emitter that partially transmits 185 nm ultraviolet (UV) emission from the lamp, dissolved dioxygen in the spray solution was converted into ozone, which subsequently cleaved the double bonds within fatty acyls of lipids. Solvent conditions, such as presence of water and acid solution pH were found to be critical in optimizing ozonolysis yields. Fast (on seconds time scale) and efficient (50–100% yield) ozonolysis was achieved for model unsaturated phospholipids and fatty acids with UV-lamp induced ozonolysis incorporated on a static and an infusion nanoESI source. The method was able to differentiate double bond location isomers and identify the geometry of the double bond based on yield. The analytical utility of UV-lamp induced ozonolysis was further demonstrated by implementation on a liquid chromatography (LC)-MS platform. Ozonolysis was effected in a flow microreactor which was made from ozone permeable tubing, so that ambient ozone produced by the lamp irradiation could diffuse into the reactor and induce online ozonolysis post-LC separation and before ESI-MS.

### Graphic Abstract

Address reprint requests to: Prof. Yu Xia, Department of Chemistry, Tsinghua University, Beijing, China, 100084, xiayu@mail.tsinghua.edu.cn.

<sup>#</sup>Current address: Intel Corporation, Hillsboro, OR 97214

## UV Induced Ozonolysis



### Keywords

ozonolysis; unsaturated lipid; electrospray ionization; lipidomics; LC-MS

## INTRODUCTION

Lipids have gained increased interest in biomedical fields in recent years as mounting evidence indicates their critical function in cell signaling [1, 2] and as biomarkers of health and disease [3]. There are also wide industrial and consumer applications for using lipids as chemical feedstocks [4], surfactants [5], and nutraceuticals [6]. Accompanying these advances, the demand is surging for accurate and rapid identification of lipids of interest from complex mixtures. Mass spectrometry (MS) based techniques have emerged as powerful methods for lipid analysis, with electrospray ionization (ESI) being commonly employed as the ionization method due to its ability to ionize a large spectrum of lipids with different physical/chemical properties and due to its compatibility with liquid chromatography (LC) separations [7, 8].

A long-standing issue with mass spectrometry based analysis is the resolution of molecular isomers, which is exacerbated in lipid analysis due to large structural diversity [9]. A well-encountered situation is determination of alkene positional and geometric isomers in lipid fatty acyls, which often requires a battery of analytical methods. For instance, conjugated linoleic acids (CLAs), which are found to have health benefits including weight reduction and cancer prevention among others, typically exist in several isomeric forms [6]. The most abundant naturally occurring CLA is FA18:2 (9Z, 11E) with many other isomers existing in low abundance [10]. Although gas chromatography (GC) and silver ion liquid chromatography can separate most isomers of CLA fatty acid methyl esters, complete

structural characterization of individual isomers requires collective efforts from MS, nuclear magnetic resonance, and Fourier transform infrared spectroscopy [11].

Recently there have been promising developments in MS, aiming to address the analytical challenge of carbon-carbon double bond (C=C) characterization with simplified procedures, increased sensitivity and throughput. These include solution derivatization (ozonolysis [12], the Paternò-Büchi reaction [13, 14], charge-switch derivatization [15], etc.), new gas-phase ion activation/dissociation methods (charge remote fragmentation [16, 17], ion/molecule reactions [18], radical-based dissociation [19, 20], electron-based excitation [21], ultraviolet photo-dissociation [22, 23], etc.), and coupling ion mobility separation with MS [24–26]. Among these, ozonolysis of unsaturated fatty acyls has historically been a reliable method for locating C=C by detecting the aldehyde products [27, 28]. During ozonolysis, ozone reacts with the alkene functional group to form a primary ozonide which rapidly dissociates to a site specific aldehyde and a carbonyl oxide (Criegee intermediate) [29]. The products can then recombine to form secondary ozonides or the Criegee intermediate subsequently reacts with adjacent solvent molecules. In the past decade ozonolysis has been adapted to ESI-MS and applied to glycerophospholipids (GPs), glycerolipids (GLs), and fatty acid methyl esters (FAMES) [12, 30]. Online ozonolysis ESI has been implemented by via corona discharge at the ESI tip region, adding ozone to the ESI desolvation gas (ozone ESI), and ionization via low temperature plasma ionization at ambient air [31–33]. Direct information can be obtained on the lengths of chains being cleaved off at each C=C from the unsaturated fatty acyls. Because it is necessary to link the ozonolysis products to their intact precursors to achieve C=C location determination, ozone ESI is not well suited for complex lipid mixture analysis. To solve this problem, the Blanksby group subsequently implemented ion/molecule (ozone) reactions to achieve ozonolysis of mass-selected ions inside a mass spectrometer, termed OzID, which has been demonstrated for complex mixture analysis on different instrument platforms [34–38]. Alternatively, the Curtis group demonstrated in-line ozonolysis after 1 or 2-dimensional LC separations prior to MS analysis. Due to excellent lipid separation with LC, identification of geometric and positional lipid isomers of conjugated CLA FAMES and GPs in complex mixtures have been achieved [39–41].

In the above-mentioned ozonolysis applications, dedicated ozone generators have been used as sources for ozone production. These ozone generators utilize dielectric barrier discharge or corona discharge of dioxygen gas to achieve high ozone concentrations (up to 10%) [42]. Photodissociation of dioxygen by vacuum UV (VUV) photons is an alternative method to generate ozone. For instance, low pressure mercury (LP Hg) lamps are known as “ozone producing” lamps when the emission wavelength at 185 nm is not filtered. Photodissociation of dioxygen at 185 nm results in the production of two O (<sup>3</sup>P) atoms. The O (<sup>3</sup>P) atom then combines with molecular oxygen to form ozone in the presence of a non-reacting species (Figure 1a). Resulting from irradiation by the 254 nm wavelength emission of the LP Hg lamp, a significant portion of ozone decomposes into O (<sup>1</sup>D) and O<sub>2</sub> and ozone concentrations are reported to reach 0.001 % in ambient air [43]. Although producing much lower concentrations of ozone as compared to the ozone generators, LP Hg lamps enjoy advantages of low power consumption, small physical size, and wide accessibility (commercially available at relatively low cost). Considering the traits of LP Hg lamps, we attempted to develop an ozonolysis reactor which could be coupled online with ESI-MS by

employing an LP Hg lamp for ozone production. Using unsaturated lipid standards (FAs and GPs), including their C=C location isomers and configuration isomers as model compounds, we demonstrated that UV induced ozonolysis from an LP Hg lamp in ambient air was highly efficient and could be online coupled with ESI from nanoflow to microflow regimes. The compatibility of the online ozonolysis reactor with LC-ESI-MS was further demonstrated using a mock mixture of unsaturated FA isomers.

## Experimental

### Lipid Nomenclature

Shorthand notation from the Lipid Maps project was used for lipid structural identification [44, 45]. For GP standards, the head group, fatty acyl stereo position, fatty acyl carbon number, degree of unsaturation, and alkene stereo orientation were specified. For example, PE 16:0/18:1(9Z) signifies the glycerophosphoethanolamine head group with 16 and 18 carbon fatty acyl chains on the *sn1* and *sn2* glycerol positions, respectively. The “0” and “1” after the carbon number refers to the degree of unsaturation of the respective fatty acyl. Alkene bond location was defined by counting sequential carbons starting from alpha carbon of the fatty acyl ester and proceeding towards the terminal carbon, *i.e.* C=C bond at the 9 position is located between carbon 9 and 10 of the fatty acyl. Z and E nomenclature for alkene bond stereo configuration follows the alkene location identifier.

### Chemicals

1-palmitoyl-2-oleoyl-*sn*-glycero-3-phosphocholine (PC 16:0/18:1(9Z)) and 1-stearoyl-2-oleoyl-*sn*-glycero-3-phosphate (PA 18:0/18:1(9Z)) dissolved in 10 mg/mL chloroform were purchased from Avanti Polar Lipids, Inc. (Alabaster, AL, USA). Stock solutions in chloroform were diluted with isopropanol (LC grade; Macron Fine Chemicals; Center Valley, PA, USA) before diluting to the final working solution. Primary organic solvents used in ESI working solutions were all LC grade and consisted of methanol (Macron Fine Chemicals), acetonitrile (Sigma Aldrich; St. Louis, MO, USA), and isopropanol. Ultrapure H<sub>2</sub>O was obtained from a purification system at 0.03 μS-cm (model: Micropure UV; Thermo Scientific; San Jose, CA, USA). Ammonium hydroxide (28–30% as NH<sub>3</sub>; Macron Fine Chemicals), glacial acetic acid (Mallinckrodt Chemicals; Hazelwood, MO, USA), formic acid and ammonium formate (Sigma Aldrich, St. Louis, MO, USA) were used as solution modifiers to enhance lipid ionization via ESI. 1-Stearoyl-2-arachidonoyl (PC 17:0/20:4), *cis*-vaccenic acid (FA 18:1 (11Z)), and oleic acid (FA 18:1 (9Z)) were purchased as purified oils and dissolved in chloroform for final concentrations of 1 mg/mL and subsequently diluted into working solutions.

### NanoESI

Ozonolysis was effected with two different nanoESI sources made from fused silica capillary or borosilicate glass. Fused silica tips were purchased prefabricated from New Objective, Inc. (Woburn, MA, USA) and were connected to a stainless-steel union (Valco; Houston, TX, USA) which served to join the solution propelled by syringe pump (Harvard Apparatus; Holliston, MA, model: 11 plus) to the nanoESI emitter and was also the point of high voltage application to effect electrospray (~ ±1.5 kV). Borosilicate glass tips were made

from capillary (1.5 mm o.d. and 0.86 mm i.d.) pulled to a ~10  $\mu\text{m}$  i.d. tip using a micropipette puller (P-1000 Flaming/Brown; Sutter Instrument, Novato, CA, USA). A stainless-steel wire (~4 cm in length) was inserted through the back of the tip and was in contact with the sample fluid. High voltage DC potential of  $\sim \pm 1.5$  kV was applied between the source and MS inlet which enabled a stable ion current via electroosmotic flow of ~20 nL/min.

### Ozone reactions

A 20 mA, 2.54 cm lamp length, 0.64 cm diameter, double bore tubing low pressure mercury (LP Hg) lamp (model number: 81-1057-51; BHK, Inc.; Ontario, CA) was used to create ozone. Lamp specifications from the manufacturer state the emission intensities at 20 cm distance for 254 and 185 nm is 73 and 42  $\mu\text{W}/\text{cm}^2$ , respectively (185 nm intensity measured in argon atmosphere). For most experiments the lamp was positioned vertically and 0.5–1.5 cm orthogonal from the emitter tip depending on the experiment with more details described in the Results and Discussion. Ozone concentration under ambient conditions was measured using an ozone analyzer (model 49i; Thermo Scientific).

### Mass Spectrometry

All data were collected on a 4000 QTRAP mass spectrometer (Sciex, Toronto, Canada) equipped with a home-built nanoESI source. The characteristic parameters of the mass spectrometer using in this study were set as follows: spray voltage,  $\pm 1200 - \pm 1500$  V; curtain gas, 10 psi; and declustering potential,  $\pm 40$  V. Data acquisition, processing, and instrument control were performed using Analyst 1.5 software.

### Online ozonolysis-LC-MS for fatty acid mixture analysis

The LC system consisted of a binary pump (Agilent 1200, Waldbronn, German) and a manual injector with a 10  $\mu\text{L}$ -sample loop. A C18 column (150 mm  $\times$  4.6 mm i.d., 5  $\mu\text{m}$  particle size, Agilent) was used for chromatographic separation. An ozone reactor was made by ozone permeable Teflon AF-2400 tubing (0.02-inch o.d., 0.01-inch i.d., 80-cm in length; Biogeneral Inc., CA, USA). The AF tubing was coiled concentrically at 3 cm radius with the UV lamp placed in the center. The reactor connected the LC and a homemade splitter (1:50 v/v), which decreased the flow rate to 10  $\mu\text{L}/\text{min}$  for ESI-MS. Mobile phase consisted of acetonitrile with 0.5% formic acid (v/v, A) and ammonium formate buffer (10 mM, B). Gradient elution was used as follows: 80% B (5 min), 80–85% B (5–10 min), 85–90% B (10–15 min) and 95–100% B (22 min). At the end of elution, the gradient was set back to 80% B and the system was allowed to equilibrate.

## Results and Discussions

The formation of ozone from an LP Hg lamp used in this study was monitored by an ozone analyzer via photometric detection, sampling at 1 cm distance from the lamp. Ozone concentration was found around 10 ppm (data not shown). We then placed the lamp 0.5 cm away from a static-nanoESI emitter made from a pulled borosilicate glass tip to test if efficient ozonolysis can be implemented at the nanoESI-MS interface. Figure 1c and 1d compare the nanoESI MS spectra of an unsaturated model lipid, PC 16:0/18:1(9Z) (5  $\mu\text{M}$  in

7:3 ACN: H<sub>2</sub>O, 1% acetic acid) before and during UV irradiation in positive ion mode. Before the lamp was turned on, protonated PC ([M+H]<sup>+</sup>, *m/z* 760.6) was detected as the most abundant species accompanied by a small sodium adduct peak (*m/z* 782.4). Upon UV irradiation, the intact PC signal dropped significantly, while a peak at *m/z* 650.4 appeared, corresponding to cleavage of the 9 C=C and formation of an aldehyde at this position (structure shown in Figure 1e). Combining the information from ozonolysis with that obtained from conventional MS/MS experiments, relatively complete structural information of this lipid molecule, including the head group (obtained from CID in the positive ion mode), fatty acyl chain composition (obtained from CID in the negative ion mode), and C=C location, can thus be determined.

Figure 1f shows the extracted ion chromatogram (XIC) of intact PC (*m/z* 760.6) and the ozonolysis product (*m/z* 650.4) for two consecutive events when the lamp was turned on for 12 s and subsequently turned off. With the lamp on, the precursor ion was converted approximately 100% to *m/z* 650.4 and the intact PC was completely consumed. After the lamp was turned off, ozonolysis product was observed for approximately 2 minutes, suggesting that most of the reaction occurred in solution near the spray tip. Ozone might be formed from two sources: (1) formation in the tip due to trace oxygen dissolved in the solution or (2) diffusion of ozone from the spray plume region into the solution through the tip. Borosilicate glass does not transmit UV photons of wavelengths shorter than 250 nm due to the presence of additives in glass; however, the glass thickness near the tip approaches micrometer dimensions which increases the likelihood of photon transmission to the solution. On the other hand, it has been reported that dioxygen can diffuse into the solution from the ESI tip which is exposed to atmospheric pressure [46]. Given the low flow rate that the static nanoESI operates (around 20 nL/min), it is possible that ozone formed at the vicinity of the tip can effectively diffuse into the nanoESI solution and react with the unsaturated lipid alkene.

The UV-lamp induced ozonolysis setup was further tested for unsaturated phospholipid analysis in negative ion mode. Figure 2a shows the reaction spectrum of PA 18:0/18:1(9Z) prepared at 5 μM in 1:1 ACN:MeOH with 1% acetic acid added upon UV irradiation. Two major reaction products were observed at *m/z* 591.5 and 639.5, respectively. Product at *m/z* 591.5 is the aldehyde formed from cleavage of the 9 C=C. Product at *m/z* 639.5 is 48 Da higher in mass than the aldehyde product, characteristic for the formation of the α-methoxyhydroperoxide product (structure motif shown in the inset of Figure 2a). This product results from reaction between methanol and the Criegee intermediate and has been previously demonstrated when methanol is used as a co-solvent for in-source ozonolysis-MS experiments [32]. Detection of α-methoxyhydroperoxide product provided strong evidence that ozone was indeed involved in unsaturated lipid alkene cleavage and site-specific aldehyde formation for the reactions reported in this study.

Figure 2b demonstrates the application of UV-lamp ozonolysis for the analysis of lipid molecules consisting of polyunsaturated fatty acyls. The nanoESI spray solution of PC 17:0/20:4 (5Z,8Z,11Z,14Z) was prepared at 10 μM in 69:30:1 ACN:H<sub>2</sub>O:MeOH with 1% acetic acid added. As shown in the reaction spectrum (Figure 2b), the aldehyde products are formed abundantly, viz. ions at *m/z* 608.4, 648.4, 688.5, and 728.5, resulting from

ozonolysis at the 5, 8, 11, and 14 double bonds. Minor  $\alpha$ -methoxyhydroperoxide products were also detected (not labeled) due to the presence of 1% MeOH in the solution. This experiment suggests UV-lamp induced ozonolysis is applicable for alkene localization in polyunsaturated lipids.

Being successful in coupling UV-lamp induced ozonolysis on a static nanoESI source, we further tested its compatibility with infusion nanoESI operating in a higher flow rate regime (300 nL/min to 1  $\mu$ L/min). Figure 3a shows schematics of the experimental setup. The nanoESI emitter (15  $\mu$ m tip i.d.) was constructed from fused silica capillary (75  $\mu$ m tip i.d.) with polyamide coating removed from the tip (~7 mm) during manufacturing. The LP Hg lamp was placed at 1.5 cm away from the tip. Oleic acid (FA 18:1(9Z)), consisting of a single C=C in the fatty acyl chain, was used a model compound. Figure 3b shows the MS spectrum of 5  $\mu$ M oleic acid prepared in 7:3 ACN:H<sub>2</sub>O (0.5% formic acid added) infused at 500 nL/min in negative ion mode. The deprotonated oleic acid peak ([M-H]<sup>-</sup>) was clearly detected at  $m/z$  281.4. When the lamp was turned on, the ozonolysis product at  $m/z$  171.3 which would be consistent for C<sub>9</sub>H<sub>15</sub>O<sub>3</sub><sup>-</sup> immediately appeared, corresponding to deprotonated 9-oxo-nonanoic acid (Figure 3c). This product allowed identification of the alkene functional group between C9–C10, counting from the carboxylic acid side [47].

Turning the lamp on and off the process of C=C cleavage and 9-oxo-nonanoic acid ion formation can be activated or deactivated, respectively, on the seconds timescale. Figure 3d represents an XIC of intact oleic acid ([M-H]<sup>-</sup>,  $m/z$  281.4) and the ozonolysis product ( $m/z$  171.3) from a sequence of 3 s lamp on / 2 s lamp off (manually repeated six times) in a span of 30 s. Note that there was approximately 0.5 s delay for the lamp to warm up, resulting in approximately 2.5 s effective illumination time. With the lamp on for 2.5 s the oleic acid ion intensity decreased to 1.35e6 counts per second (cps) from 3.8e6 cps, accounting for 65% decrease in intensity (Figures 3b and 3c are the corresponding MS<sup>1</sup> spectra). Simultaneously, the 9-oxo-nonanoic acid ion increased to 50% the original oleic acid ion intensity before UV exposure. When the lamp was turned off the ion signal at  $m/z$  171.3 began to decrease while  $m/z$  281.4 increased, clearly demonstrating that the peaks were affected by irradiating the fused silica nanoESI tip with UV light from the lamp. When the experiment was completed after 32 s the precursor signal at  $m/z$  281.4 returned to its original intensity. At 500 nL/min solution flow rate and 7 mm exposure length the solution traverses this length in 3.7 s. Upon close observation of the XIC in Figure 3d, the ozonolysis product ( $m/z$  171.3) lasted for ~ 4.2 s after the lamp was turned off. This timing indicates that the majority of the ozonolysis occurs in solution, which likely results from ozone formation from oxygen dissolved in the solution. When N<sub>2</sub> purged solution was subjected to the same experiments, the yield of 9-oxo-nonanoic acid was significantly reduced. The remaining small amount of ozonolysis product was caused by ambient oxygen diffused into the ESI solution through the tip opening. Similarly, experiments at the same flow rate but using a stainless-steel nanoESI source also resulted in drastically reduced yield of 9-oxo-nonanoic acid ion, further corroborating the hypothesis of solution ozonolysis. Using the fused silica nanoESI setup, UV-lamp induced ozonolysis was achieved in reasonable yields (>50%) for flow rate from 300–1000 nL/min.

### Effect of water in the solvent for ozonolysis

Beauchamp group studied the interfacial ozone reactions of oleic acid (FA 18:1(9Z)) with field-induced droplet ionization and reported detection of abundant azeleic acid ( $m/z$  187) besides 9-oxo-nonanoic acid ion ( $m/z$  171) and oleic acid dimers [47]. It was hypothesized that azeleic acid ( $\text{HOOC}(\text{CH}_2)_7\text{COOH}$ ) was a product resulting from the Criegee intermediate. Interestingly, this product was not detected in this work. Instead, the aldehyde was observed as the only ozonolysis product for lipid samples dissolved in ACN/ $\text{H}_2\text{O}$  solvent system (Figure 1d and Figure 3c). We attributed this phenomenon to presence of water in the solution. It has been reported that nucleophilic addition of water to the alpha carbon of the Criegee intermediate releases  $\text{H}_2\text{O}_2$  and forms an aldehyde (Scheme 1) [48]. Because only aldehydes are formed from ozonolysis, the reaction spectra are simple, leading to higher sensitivity for detection and straightforward elucidation of C=C location.

### Impact of solution pH

In the course of exploring optimal conditions for ozonolysis, we found it was critical to keep solution pH low. For instance, when FA or PA solutions were added with 1% ammonium hydroxide, a common additive for negative ion mode ESI, no obvious ozonolysis products were observed. It has been shown that hydroxide anion ( $\text{OH}^-$ ) reacts with ozone at rate constant in the range of  $48\text{--}70 \text{ M}^{-1}\text{s}^{-1}$  (Reaction, 1) [49]. At basic solution pH, the half-life of ozone in solution decreases significantly, resulting in negligible alkene cleavage products. The replacement of ammonium hydroxide by 1% acetic acid indeed improved ozonolysis to ~15% yield for oleic acid solution upon UV irradiation. Interestingly, addition of 0.5% formic acid in the solution (in place of acetic acid) produced higher yield ozonolysis (~60%, Figure 3c). The pKa of formic acid is 3.75 relative to 4.75 of acetic acid, corresponding to theoretical pH values of 2.3 and 2.7, respectively, for compositions of 0.5% formic acid and 1% acetic acid in 1 mL aqueous solution. For GPs, it was experimentally determined that addition of 1% acetic acid to the ESI solution produced abundant aldehyde reaction products, therefore not requiring the use of formic acid. It is not clear at this time exactly why ozonolysis of GPs is more efficient at higher pH relative to FAs. However, it is evident that conditions of low pH are critical for efficient ozonolysis and this could be due to the relatively low concentration of ozone produced with the LP Hg lamp used in this study.



### Other possible reactions

In addition to ozonolysis, we acknowledge the complex chemistry/photochemistry which occurs in solution from UV radiation and therefore do not rule out the possibility of other mechanisms for the observed alkene cleavages. The 185 nm emission from an LP Hg lamp can also be absorbed by  $\text{H}_2\text{O}$  in the solution phase resulting in photodissociation producing hydroxyl radical, a process which is used extensively in water purification [50]. The concentration of dioxygen in solution is approximately 2 mM and a solution containing 30%  $\text{H}_2\text{O}$  has an  $[\text{H}_2\text{O}]$  of 17 M. Lipid peroxidation with hydroxyl radical typically involves rearrangement of the alkene upon hydrogen abstraction and oxygen addition [51]. The



related reaction products were not observed when performing the reaction with standard lipids, which provides evidence that hydroxyl radical was not ultimately involved in alkene cleavage. In addition, alkene functional groups absorb UV radiation where conjugated double bonds are sensitive to ~233 nm wavelength while mono and polyunsaturated species absorb below 200 nm wavelength. Bond geometry isomerization and subsequent photochemical reactions are common events following photon absorption [52]. Irradiation of ESI solution containing unsaturated lipids with UV light from a LP Hg lamp could potentially result in direct photon absorption by the alkene functional group. These photochemical reactions appear though to not have a significant impact during the UV-induced ozonolysis as evidenced by the minimal observation of side reaction products. The geometry of *cis*/ *trans* isomers also appears to be conserved through observation of different ozonolysis reaction rates (to be discussed in subsequent sections).

### Analysis of mixtures of C=C location isomers

FAs having the same number of carbons but with different alkene locations are termed positional isomers and during mixture analysis cannot be resolved with MS or MS/MS at low CID energy conditions. Ozonolysis is a powerful method for determining C=C location and can be utilized for isomer differentiation. To demonstrate this ability, a mixture of oleic acid (FA 18:1(9Z)) and *cis*-vaccenic acid (FA 18:1(11Z)) (5  $\mu$ M each in 7:3 ACN:H<sub>2</sub>O, 0.5% formic acid added) was subjected to UV-induced ozonolysis using the static nanoESI setup. Figure 4a shows the reaction spectrum, in which the aldehyde products of each isomer are observed abundantly at  $m/z$  171.2 and 199.2 besides the remaining intact FA ions ( $m/z$  281.4). The aldehyde ions provide direct evidence for locating C=C at 9 and 11, respectively, which otherwise would not be obtainable on standard ESI MS/MS platforms. In addition to identification, there is the potential for relative isomer quantitation based on intensity ratios of ozonolysis products. Figure 4b shows such a plot as a function of *cis*-vaccenic/oleic acid molar ratios while keeping the total concentration of *cis*-vaccenic and oleic acid at a constant 10  $\mu$ M. A linear relationship ( $R^2 = 0.9925$ ) was obtained for the FA 18:1(11Z)/FA 18:1(9Z) molar ratios ranging from 0.075–13.3 and the limit of detection for each isomer in the mixture was 0.2  $\mu$ mol.

Conjugated linoleic acids (CLA) are a widely studied class of natural and synthetically derived FAs which have potential human health benefits including anti-cancer properties [6]. Online ESI MS ozonolysis of CLA FAMES has been demonstrated in both the solution and gas phase with ozone generators [41, 53]. Figure 4c shows UV-lamp induced ozonolysis of a mixture of two CLA isomers, FA 18:2(9Z, 11E) and FA 18:2(10E, 12Z) ( $[M-H]^-$ ,  $m/z$  279.3). The aldehyde products at  $m/z$  171.2 and 197.2 derived from ozonolysis of FA 18:2(9Z, 11E), while ions at  $m/z$  185.2 and 211.2 resulted from FA 18:2 (10E, 12Z). Peaks at  $m/z$  295.4 and 313.5 are sequential oxidation reaction products from the CLA precursor while all other ions were present before application of UV and are considered as background. In the literature it is reported that *trans*-double bonds have faster ozonolysis reaction kinetics relative to the *cis*-geometry [35, 54]. This phenomenon was indeed observed during UV-lamp induced ozonolysis. For instance, the intensity of the 11E ( $m/z$  197.2) and 10E ( $m/z$  185.2) products are higher than the 9Z ( $m/z$  171.2) and 12Z ( $m/z$  211.2), respectively. Based on the ozonolysis reaction rate difference, the intensity

differences between *cis*/*trans* geometries may be used to identify alkene geometries during analysis of unknown samples. Furthermore, observation of the different reaction rates between *cis*- / *trans*-geometries gives further indication that, at least during initial stages of UV-lamp induced ozonolysis, geometry is conserved during UV induced ozonolysis.

### Coupling UV-lamp induced ozonolysis with online LC-MS

The Curtis group has successfully demonstrated coupling an ozonolysis reactor in-line with LC-MS for locating double bond positions in lipid mixtures (FAMES and PCs) [39–41]. In their studies, the reactor is produced from thin-walled (0.02-inch o.d., 0.01-inch i.d.) Teflon AF-2400 tubing, which passes through a bottle filled with gaseous ozone at  $35.6 \text{ g m}^{-3}$  (~2.5%). Ozone can diffuse into the tubing due to semi-permeable nature of the material and react with unsaturated lipids efficiently in solution at even relatively high flow rate (~0.5 mL/min) prior to ionization and MS analysis. Inspired by their work, we also tested coupling UV-lamp induced ozonolysis with online LC-MS. Figure 5a shows the schematic representation of the flow reactor placed in after the LC column and before a home-built ESI source. The flow reactor was made from the same Teflon AF-2400 tubing, which was concentrically coiled (80 cm in length) at 3-cm radius, while the UV lamp (185 nm) was placed in the center. The distance between the coil and the lamp was about 2.5 cm. At a flow rate of 0.5 mL/min, the effective reaction time was 15 s, equivalent to the residence time of the solution traveled in the UV exposed region of the tubing. A mock mixture of four unsaturated fatty acids, including FA 18:2 (9Z, 12Z), FA 18:2 (10E, 12Z), FA 17:1 (10Z) and FA 18:1 (9Z) was subjected to reversed-phase LC separation, post-column ozonolysis, and ESI-MS analysis. As shown in the ion chromatogram (Figure 5b), all five species were well separated, even for the C=C location isomers, FA 18:2 (9Z, 12 Z) and FA 18:2 (10E, 12Z). Figure 5c–f present the ozonolysis spectra (negative ion mode) of each fatty acid eluent. The aldehyde products corresponding to cleavage of each individual C=C in the fatty acid were clearly detected, allowing confident assignment of C=C location. Compared to the inline ozonolysis reactor developed by the Curtis group, UV-lamp induced ozonolysis from our work showed lower reaction efficiency. We attributed this to high solution flow rate (0.5 mL/min) which resulted in inefficient interaction between ozone and lipids and low ozone concentration (10 ppm) produced in the current setup. Reaction efficiency could be improved by using a higher power UV lamp or multiple UV lamps. It is also worth mentioning that the low power UV-lamp is well suited for nanoflow and microflow LC-MS systems as demonstrated by data in Figures 2 and 3.

### Conclusions

In this study a low power (6 W) LP Hg lamp has been employed to facilitate ozonolysis in solution, which allows its direct coupling with static or infusion nanoESI and implementation on an LC-ESI-MS platform. Ozone formation is initiated by 185 nm UV emission from the lamp via the well-studied dioxygen photolysis pathway. To effect ozonolysis on the static (20 nL/min) and infusion (300–1000 nL/min) nanoESI sources, the lamp just needs to be placed near the spray tip region. In those two setups, experimental data prove that majority of ozonolysis happens in solution at the tip region of a nanoESI emitter. The presence of trace oxygen in spray solution and partial transmission of 185 nm UV

photon by the material made for those nanoESI emitters (thin borosilicate glass and fused silica capillary without polyamide coating) are responsible for the reactions. Using unsaturated fatty acids and phospholipids as model compounds, efficient ozonolysis (yield: 50–100%) has been achieved regardless the geometry of the C=C, degree of unsaturation, and polarity of ionization using above two nanoESI sources. Given relatively low concentrations of ozone generated by the lamp, optimal solution condition is key to obtaining high reaction yields. It is important to include water in the solvent system, e.g. ACN/H<sub>2</sub>O (7/3, v/v). This is because solvent water converts Criegee intermediate to aldehyde, consolidating other possible ozonolysis products into aldehydes. This phenomenon not only simplifies spectral interpretation for locating C=C positions but also increases detection sensitivity. The role of low pH condition is to keep [OH<sup>-</sup>] concentration low, so as to reduce side reactions between ozone and OH<sup>-</sup>. Besides nanoESI, a flow microreactor made from Teflon tubing which is permeable to ozone formed in ambient air has been developed for coupling UV-lamp induced ozonolysis directly with LC-MS. A mock mixture of unsaturated fatty acids was used as a proof-of-principle demonstration on the capability of assigning C=C location in each FA (including isomers) via base-line separation of FAs from the mixture, online ozonolysis, and subsequent ESI-MS detection. Overall, UV-lamp induced ozonolysis has attractive analytical features such as easy to implement, not instrument vendor specific, no modifications on MS needed, and low cost. However, it also inherits the same limitations as other ozoneESI techniques, including the need of a prior separation of lipid species since ozonolysis occurs in the ESI solution. UV lamp allows fast “on/off” ozonolysis on the seconds time scale (data in Figure 3). This feature although not demonstrated herein, could be useful for LC-MS platform, where the “off” cycle can be used to for identifying lipid structural information such as head group and fatty acyl composition via linked scans (MS/MS), while the “on” cycle could lead to the C=C location information, thus allowing high level structural characterization. Due to the scope of this study, only fatty acids and phospholipids were explored for ozonolysis. These two classes of lipids have relatively high solubility in ACN/H<sub>2</sub>O solvent system for ozonolysis and the response in ESI is comparable to the commonly used CHCl<sub>3</sub>/MeOH system. In future studies, UV-lamp induced ozonolysis conditions will be tailored for analyzing neutral lipids, which might require use of a more nonpolar solvent system to enhance both solubility and response in ESI.

## Acknowledgments

Financial support from NSF CHE-1308114 and NIH R01-GM118184 is greatly appreciated. C.A.S. acknowledges the Purdue Department of Chemistry for the Emerson Kampen Fellowship Award.

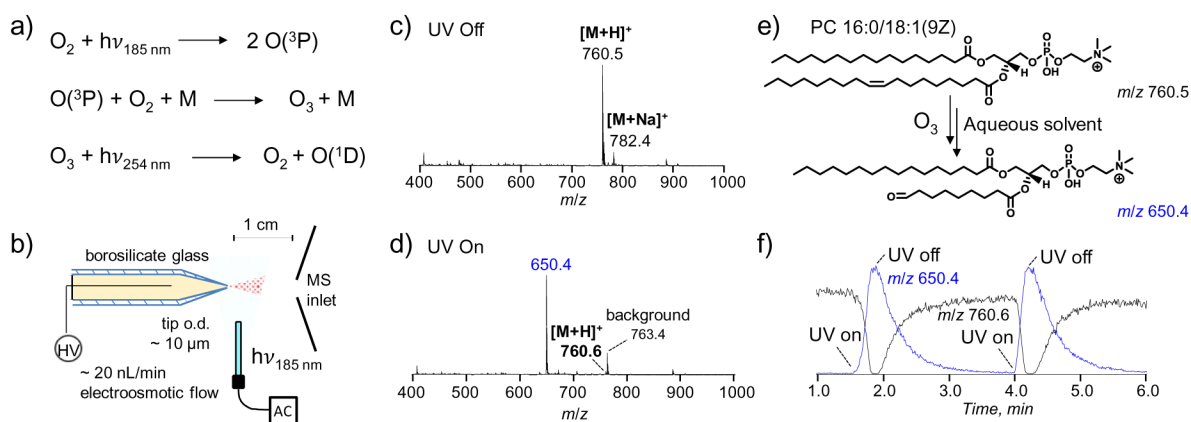
## References

1. Zeyda M, Staffler G, Hořejší V, Waldhäusl W, Stulnig TM. LAT Displacement from Lipid Rafts as a Molecular Mechanism for the Inhibition of T Cell Signaling by Polyunsaturated Fatty Acids. *J Biol Chem.* 2002; 277:28418–28423. [PubMed: 12029091]
2. Dykstra M, Cherukuri A, Sohn HW, Tzeng SJ, Pierce SK. Location Is Everything: Lipid Rafts and Immune Cell Signaling. *Annu Rev Immunol.* 2003; 21:457–481. [PubMed: 12615889]
3. Niki E. Biomarkers of Lipid Peroxidation in Clinical Material. *Biochim Biophys Acta, Gen Subj.* 2014; 1840:809–817.

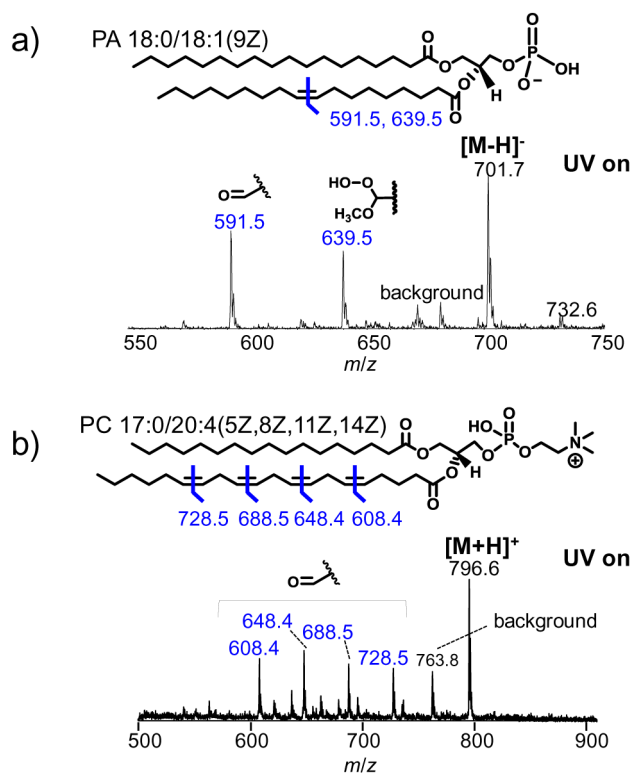
4. Mutlu H, Meier MAR. Castor Oil as a Renewable Resource for the Chemical Industry. *Eur J Lipid Sci Technol.* 2010; 112:10–30.
5. Foley P, Kermanshahi pour A, Beach ES, Zimmerman JB. Derivation and Synthesis of Renewable Surfactants. *Chem Soc Rev.* 2012; 41:1499–1518. [PubMed: 22006024]
6. Dilzer A, Park Y. Implication of Conjugated Linoleic Acid (CLA) in Human Health. *Crit Rev Food Sci Nutr.* 2011; 52:488–513.
7. Cajka T, Fiehn O. Comprehensive Analysis of Lipids in Biological Systems by Liquid Chromatography-Mass Spectrometry. *Trends Anal Chem.* 2014; 61:192–206.
8. Brügger B. Lipidomics: Analysis of the Lipid Composition of Cells and Subcellular Organelles by Electrospray Ionization Mass Spectrometry. *Annu Rev Biochem.* 2014; 83:79–98. [PubMed: 24606142]
9. Hancock SE, Poad BLJ, Batarseh A, Abbott SK, Mitchell TW. Advances and Unresolved Challenges in the Structural Characterization of Isomeric Lipids. *Anal Biochem.* 2017; 524:45–55. [PubMed: 27651163]
10. Kramer JK, Cruz-Hernandez C, Deng Z, Zhou J, Jahreis G, Dugan ME. Analysis of Conjugated Linoleic Acid and Trans 18:1 Isomers in Synthetic and Animal Products. *Am J Clin Nutr.* 2004; 79:1137S–1145S. [PubMed: 15159247]
11. Roach JAG, Mossoba MM, Yurawecz MP, Kramer JKG. Chromatographic Separation and Identification of Conjugated Linoleic Acid Isomers. *Anal Chim Acta.* 2002; 465:207–226.
12. Harrison KA, Murphy RC. Direct Mass Spectrometric Analysis of Ozonides: Application to Unsaturated Glycerophosphocholine Lipids. *Anal Chem.* 1996; 68:3224–3230. [PubMed: 8797383]
13. Ma X, Xia Y. Pinpointing Double Bonds in Lipids by Paternò - Büchi Reactions and Mass Spectrometry. *Angew Chem Int Ed.* 2014; 126:2592–2596.
14. Ma X, Chong L, Tian R, Shi R, Hu TY, Ouyang Z, Xia Y. Identification and Quantitation of Lipid C=C Location Isomers: A Shotgun Lipidomics Approach Enabled by Photochemical Reaction. *Proc Natl Acad Sci USA.* 2016; 113:2573–2578. [PubMed: 26903636]
15. Yang K, Dilthey BG, Gross RW. Identification and Quantitation of Fatty Acid Double Bond Positional Isomers: A Shotgun Lipidomics Approach Using Charge-Switch Derivatization. *Anal Chem.* 2013; 85:9742–9750. [PubMed: 24003890]
16. Hsu FF, Turk J. Structural Characterization of Unsaturated Glycerophospholipids by Multiple-Stage Linear Ion-Trap Mass Spectrometry with Electrospray Ionization. *J Am Soc Mass Spectrom.* 2008; 19:1681–1691. [PubMed: 18771936]
17. Wang M, Han RH, Han X. Fatty Acidomics: Global Analysis of Lipid Species Containing a Carboxyl Group with a Charge-Remote Fragmentation-Assisted Approach. *Anal Chem.* 2013; 85:9312–9320. [PubMed: 23971716]
18. Brown SHJ, Mitchell TW, Blanksby SJ. Analysis of Unsaturated Lipids by Ozone-Induced Dissociation. *Biochim Biophys Acta, Mol Cell Biol Lipids.* 2011; 1811:807–817.
19. Pham HT, Ly T, Trevitt AJ, Mitchell TW, Blanksby SJ. Differentiation of Complex Lipid Isomers by Radical-Directed Dissociation Mass Spectrometry. *Anal Chem.* 2012; 84:7525–7532. [PubMed: 22881372]
20. Deimler RE, Sander M, Jackson GP. Radical-Induced Fragmentation of Phospholipid Cations Using Metastable Atom-Activated Dissociation Mass Spectrometry (MAD-MS). *Int J Mass Spectrom.* 2015; 390:178–186. [PubMed: 26644782]
21. Baba T, Campbell JL, Le Blanc JCY, Baker PRS. Structural Identification of Triacylglycerol Isomers Using Electron Impact Excitation of Ions from Organics (EIEIO). *J Lipid Res.* 2016; 57:2015–2027. [PubMed: 27457033]
22. Ryan E, Nguyen CQN, Shiea C, Reid GE. Detailed Structural Characterization of Sphingolipids Via 193 Nm Ultraviolet Photodissociation and Ultra High Resolution Tandem Mass Spectrometry. *J Am Soc Mass Spectrom.* 2017; 28:1406–1419. [PubMed: 28455688]
23. Klein DR, Brodbelt JS. Structural Characterization of Phosphatidylcholines Using 193 nm Ultraviolet Photodissociation Mass Spectrometry. *Anal Chem.* 2017; 89:1516–1522. [PubMed: 28105803]

24. Bowman AP, Abzalimov RR, Shvartsburg AA. Broad Separation of Isomeric Lipids by High-Resolution Differential Ion Mobility Spectrometry with Tandem Mass Spectrometry. *J Am Soc Mass Spectrom.* 2017;1–10.
25. Kyle JE, Zhang X, Weitz KK, Monroe ME, Ibrahim YM, Moore RJ, Cha J, Sun X, Lovelace ES, Wagoner J. Uncovering Biologically Significant Lipid Isomers with Liquid Chromatography, Ion Mobility Spectrometry and Mass Spectrometry. *Analyst.* 2016; 141:1649. [PubMed: 26734689]
26. Castroperez J, Roddy TP, Nibbering NM, Shah V, McLaren DG, Previs S, Attygalle AB, Herath K, Chen Z, Wang SP. Localization of Fatty Acyl and Double Bond Positions in Phosphatidylcholines Using a Dual Stage Cid Fragmentation Coupled with Ion Mobility Mass Spectrometry. *J Am Soc Mass Spectrom.* 2011; 22:1552–1567. [PubMed: 21953258]
27. Privett OS, Nickell EC. Recent Advances in the Determination of the Structure of Fatty Acids Via Ozonolysis. *J Am Oil Chem Soc.* 1966; 43:393–400.
28. Beroza M, Bierl BA. Rapid Determination of Olefin Position in Organic Compounds in Microgram Range by Ozonolysis and Gas Chromatography. *Alkylidene Analysis Anal Chem.* 1967; 39:1131–1135.
29. Criegee R. Mechanism of Ozonolysis. *Angew Chem Int Ed.* 1975; 14:745–752.
30. Harrison KA, Davies SS, Marathe GK, McIntyre T, Prescott S, Reddy KM, Falck JR, Murphy RC. Analysis of Oxidized Glycerophosphocholine Lipids Using Electrospray Ionization Mass Spectrometry and Microderivatization Techniques. *J Mass Spectrom.* 2000; 35:224–236. [PubMed: 10679985]
31. Thomas MC, Mitchell TW, Blanksby SJ. Ozonolysis of Phospholipid Double Bonds During Electrospray Ionization: A New Tool for Structure Determination. *J Am Chem Soc.* 2006; 128:58–59. [PubMed: 16390120]
32. Thomas MC, Mitchell TW, Harman DG, Deeley JM, Murphy RC, Blanksby SJ. Elucidation of Double Bond Position in Unsaturated Lipids by Ozone Electrospray Ionization Mass Spectrometry. *Anal Chem.* 2007; 79:5013–5022. [PubMed: 17547368]
33. Zhang JI, Tao WA, Cooks RG. Facile Determination of Double Bond Position in Unsaturated Fatty Acids and Esters by Low Temperature Plasma Ionization Mass Spectrometry. *Anal Chem.* 2011; 83:4738–4744. [PubMed: 21539336]
34. Thomas MC, Mitchell TW, Harman DG, Deeley JM, Nealon JR, Blanksby SJ. Ozone-Induced Dissociation: Elucidation of Double Bond Position within Mass-Selected Lipid Ions. *Anal Chem.* 2007; 80:303–311. [PubMed: 18062677]
35. Pham H, Maccarone A, Campbell JL, Mitchell T, Blanksby S. Ozone-Induced Dissociation of Conjugated Lipids Reveals Significant Reaction Rate Enhancements and Characteristic Odd-Electron Product Ions. *J Am Soc Mass Spectrom.* 2013; 24:286–296. [PubMed: 23292977]
36. Kozłowski R, Campbell JL, Mitchell T, Blanksby S. Combining Liquid Chromatography with Ozone-Induced Dissociation for the Separation and Identification of Phosphatidylcholine Double Bond Isomers. *Anal Bioanal Chem.* 2015; 407:5053–5064. [PubMed: 25740545]
37. Vu N, Brown J, Giles K, Zhang Q. Ozone-Induced Dissociation on a Traveling Wave High-Resolution Mass Spectrometer for Determination of Double-Bond Position in Lipids. *Rapid Communications in Mass Spectrometry.* 2017; 31:1415–1423. [PubMed: 28590551]
38. Poad BLJ, Green MR, Kirk JM, Tomczyk N, Mitchell TW, Blanksby SJ. High-Pressure Ozone-Induced Dissociation for Lipid Structure Elucidation on Fast Chromatographic Timescales. *Anal Chem.* 2017; 89:4223–4229. [PubMed: 28252928]
39. Sun C, Zhao YY, Curtis JM. Elucidation of Phosphatidylcholine Isomers Using Two Dimensional Liquid Chromatography Coupled in-Line with Ozonolysis Mass Spectrometry. *J Chromatogr A.* 2014; 1351:37–45. [PubMed: 24894111]
40. Sun C, Zhao YY, Curtis JM. The Direct Determination of Double Bond Positions in Lipid Mixtures by Liquid Chromatography/in-Line Ozonolysis/Mass Spectrometry. *Anal Chim Acta.* 2013; 762:68–75. [PubMed: 23327947]
41. Sun C, Black BA, Zhao YY, Gänzle MG, Curtis JM. Identification of Conjugated Linoleic Acid (CLA) Isomers by Silver Ion-Liquid Chromatography/in-Line Ozonolysis/Mass Spectrometry ( $\text{Ag}^+$ -LC/ $\text{O}_3$ -MS). *Anal Chem.* 2013; 85:7345–7352. [PubMed: 23789881]

42. Chang JS, Lawless PA, Yamamoto T. Corona Discharge Processes. *IEEE Trans Plasma Sci.* 1991; 19:1152–1166.
43. Dohan JM, Masschelein WJ. The Photochemical Generation of Ozone: Present State-of-the-Art. *Ozone Sci Eng.* 1987; 9:315–334.
44. Liebisch G, Vizcaíno JA, Köfeler H, Trötz Müller M, Griffiths WJ, Schmitz G, Spener F, Wakelam MJO. Shorthand Notation for Lipid Structures Derived from Mass Spectrometry. *J Lipid Res.* 2013; 54:1523–1530. [PubMed: 23549332]
45. Fahy E, Subramaniam S, Murphy RC, Nishijima M, Raetz CRH, Shimizu T, Spener F, van Meer G, Wakelam MJO, Dennis EA. Update of the Lipid Maps Comprehensive Classification System for Lipids. *J Lipid Res.* 2009; 50:S9–S14. [PubMed: 19098281]
46. Pozniak BP, Cole RB. Ambient Gas Influence on Electrospray Potential as Revealed by Potential Mapping within the Electrospray Capillary. *Anal Chem.* 2007; 79:3383–3391. [PubMed: 17385842]
47. Grimm RL, Hodyss R, Beauchamp JL. Probing Interfacial Chemistry of Single Droplets with Field-Induced Droplet Ionization Mass Spectrometry: Physical Adsorption of Polycyclic Aromatic Hydrocarbons and Ozonolysis of Oleic Acid and Related Compounds. *Anal Chem.* 2006; 78:3800–3806. [PubMed: 16737240]
48. Schiaffo CE, Dussault PH. Ozonolysis in Solvent/Water Mixtures: Direct Conversion of Alkenes to Aldehydes and Ketones. *J Org Chem.* 2008; 73:4688–4690. [PubMed: 18505290]
49. Staehelin J, Hoigne J. Decomposition of Ozone in Water: Rate of Initiation by Hydroxide Ions and Hydrogen Peroxide. *Environ Sci Technol.* 1982; 16:676–681.
50. Zoschke K, Börnick H, Worch E. Vacuum-Uv Radiation at 185 nm in Water Treatment – a Review. *Water Res.* 2014; 52:131–145. [PubMed: 24463177]
51. Catalá A. Lipid Peroxidation of Membrane Phospholipids Generates Hydroxy-Alkenals and Oxidized Phospholipids Active in Physiological and/or Pathological Conditions. *Chem Phys Lipids.* 2009; 157:1–11. [PubMed: 18977338]
52. Adam W, Oppenländer T. 185-nm Photochemistry of Olefins, Strained Hydrocarbons, and Azoalkanes in Solution. *Angew Chem Int Ed.* 1986; 25:661–672.
53. Pham HTM, AT, Campbell JL, Mitchell TW, Blanksby SJ. Ozone-Induced Dissociation of Conjugated Lipids Reveals Significant Reaction Rate Enhancements and Characteristic Odd-Electron Product Ions. *J Am Soc Mass Spectrom.* 2013; 24:289–296.
54. Avzianova EV, Ariya PA. Temperature-Dependent Kinetic Study for Ozonolysis of Selected Tropospheric Alkenes. *Int J Chem Kinet.* 2002; 34:678–684.

**Figure 1.**

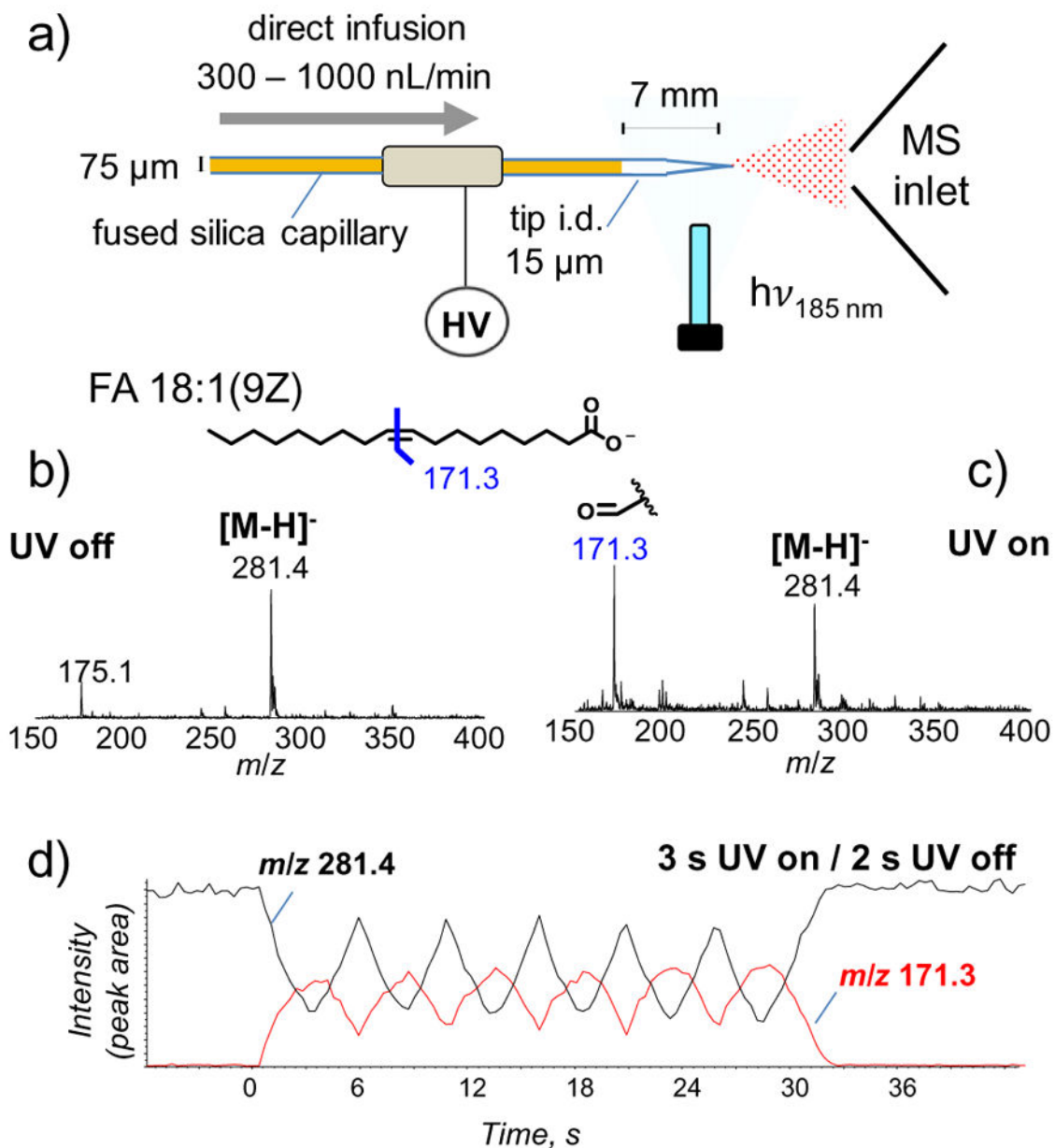
a) Ozone formation and decomposition in ambient air near an LP-Hg lamp. b) Experimental setup for implementing UV-lamp induced ozonolysis on a static nanoESI source. Positive ion mode MS spectra of 5  $\mu\text{M}$  PC 16:0/18:1(9Z) dissolved in 7:3 ACN:H<sub>2</sub>O, 1% acetic acid (c) before UV irradiation and (d) during UV irradiation. e) Structures of protonated PC 16:0/18:1(9Z) and the aldehyde product resulting from ozonolysis. (f) XIC of on/off ozonolysis depicting the baseline peak area intensities of precursor ion ( $m/z$  760.6) and reaction product ( $m/z$  650.4) as a function of time.



**Figure 2.**

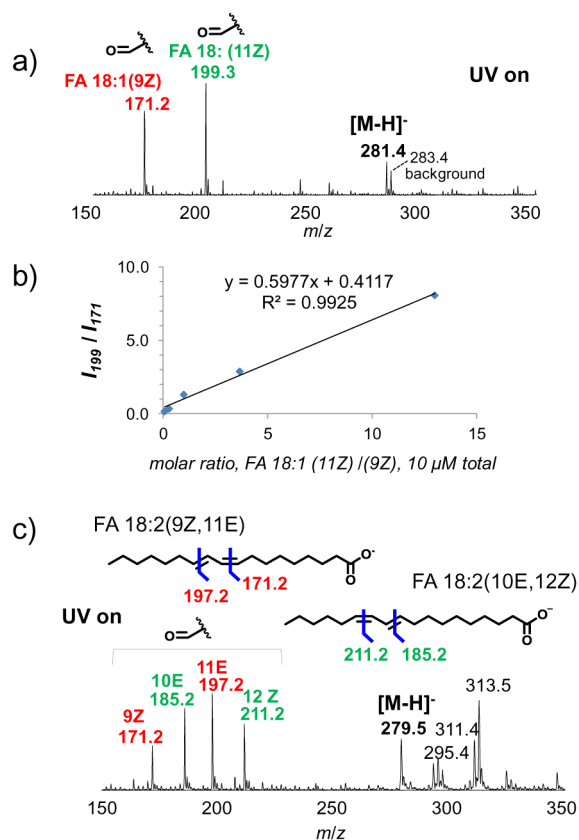
UV-lamp induced ozonolysis of unsaturated phospholipids: a) negative ion mode nanoESI of 5  $\mu$ M PA 18:0/18:1(9Z) in 1:1 ACN:MeOH with 1% acetic acid added and b) positive ion mode nanoESI of 10  $\mu$ M PC 17:0/20:4(5Z,8Z,11Z,14Z) in 69:30:1 ACN:H<sub>2</sub>O:MeOH with 1% acetic acid added. The structure motifs of ozonolysis products are indicated in figure insets.



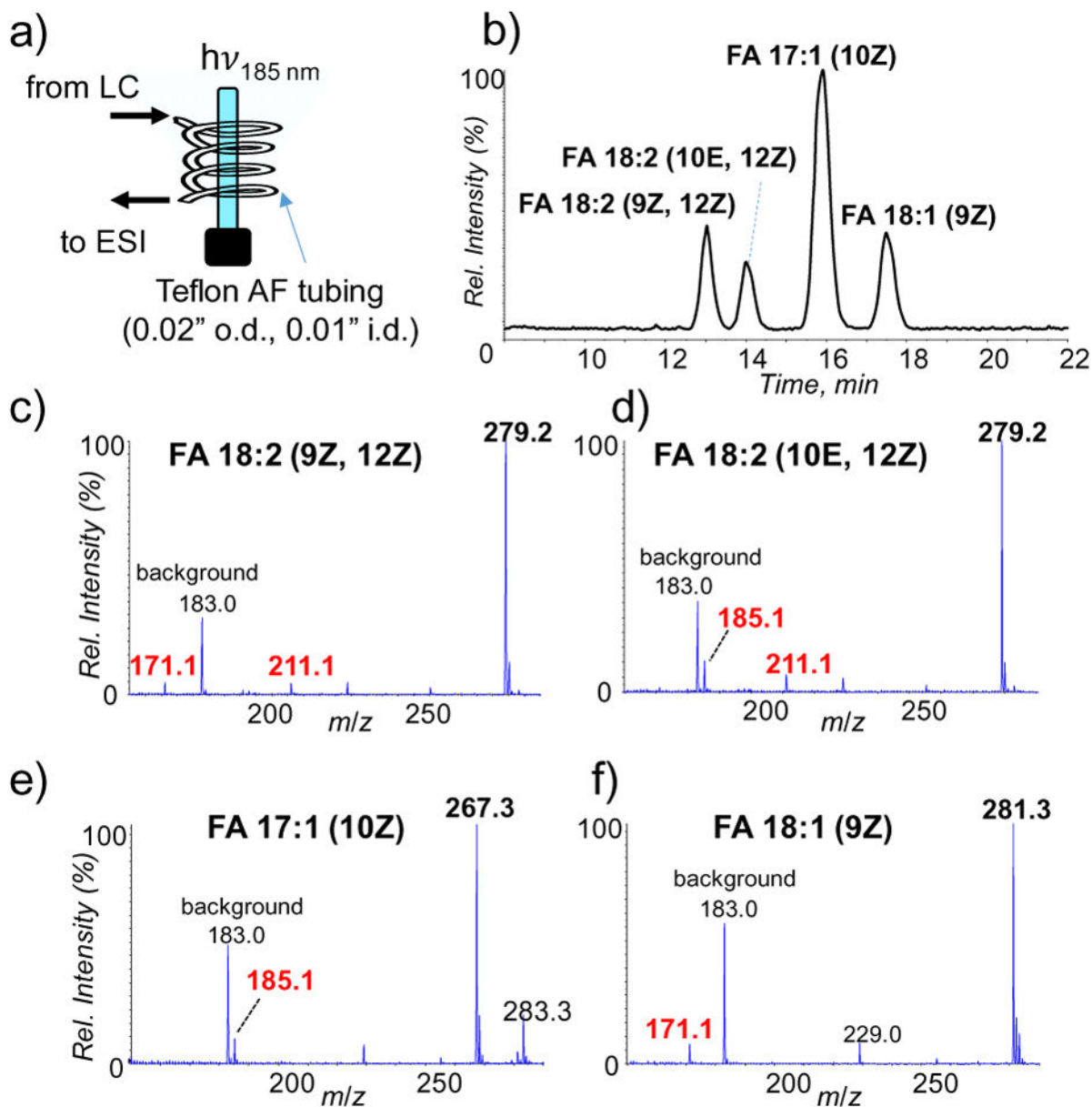


**Figure 3.**

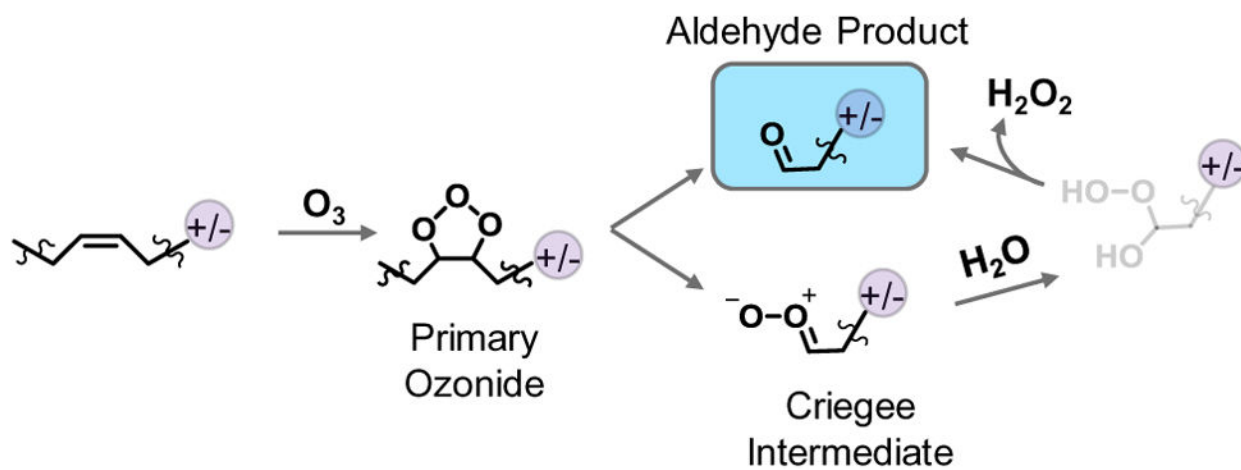
a) Schematics of the reaction setup for UV-lamp induced ozonolysis coupled with infusing nanoESI. Negative ion mode MS spectra of oleic acid (FA 18:1(9Z), 5  $\mu\text{M}$ , dissolved in 7:3 ACN:  $\text{H}_2\text{O}$ , 0.5% formic acid added) at 500 nL/min flow rate: b) before UV irradiation and c) after 2.5 s UV irradiation. d) XIC of intact oleic ion ( $[\text{M}-\text{H}]^-$ ,  $m/z$  281.4) and deprotonated 9-oxo-nonanoic acid ( $m/z$  171.3) with the lamp manually turned on for 3 s and off for 2 s sequentially.

**Figure 4.**

Application of UV-induced ozonolysis for FA C=C isomer analysis. (a) Negative ion mode MS spectrum of ozonolysis of 1:1 mixture of oleic acid (FA 18:1(9Z)) and cis-vaccenic acid (FA 18:1(11Z)). (b) A plot of ratios of aldehyde products of vaccenic/oleic acid vs. their molar concentration ratios (total of 10  $\mu\text{M}$ ). (c) Negative ion mode ozonolysis MS spectrum of a mixture of two CLA isomers, FA 18:2(9Z, 11E) and FA 18:2(10E, 12Z) ([M-H]<sup>-</sup>,  $m/z$  279.5).



**Figure 5.** UV-lamp induced ozonolysis coupled online with LC-MS for fatty acid mixture analysis. (a) Cartoon depiction of the experimental setup. (b) Reversed-phase liquid chromatogram of four unsaturated fatty acids. ESI-MS spectra in negative ion mode of (c) FA 18:2 (9Z, 12Z), (d) FA 18:2 (10E, 12Z), (e) FA 17:1 (10Z) and (f) FA 18:1 (9Z) after online ozonolysis.

**Scheme 1.**

Formation of aldehyde as the main product for ozonolysis in the presence of water as solvent. For simplicity, only the reaction product consisting of charge moiety are depicted in the scheme.